

# Searching for Gravitational Waves from the Inspiral of Precessing Binary Systems: Astrophysical Expectations and Detection Efficiency of “Spiky” Templates.

Philippe Grandclément\*

Laboratoire de Mathématiques et de Physique Théorique, CNRS-UMR 6083,  
Université de Tours, Parc de Grandmont, 37200 Tours, FRANCE and  
Northwestern University, Dept. of Physics & Astronomy, 2145 Sheridan Road, Evanston 60208, USA

Mia Ihm,<sup>†</sup> Vassiliki Kalogera,<sup>‡</sup> and Krzysztof Belczynski<sup>§</sup>

Northwestern University, Dept. of Physics & Astronomy, 2145 Sheridan Road, Evanston 60208, USA  
(Dated: December 16, 2003)

Relativistic spin-orbit and spin-spin couplings has been shown to modify the gravitational waveforms expected from inspiraling binaries with a black hole and a neutron star. As a result inspiral signals may be missed due to significant losses in signal-to-noise ratio, if precession effects are ignored in gravitational-wave searches. We examine the sensitivity of the anticipated loss of signal-to-noise ratio on two factors: the accuracy of the precessing waveforms adopted as the true signals and the expected distributions of spin-orbit tilt angles, given the current understanding of their physical origin. We find that the results obtained using signals generated by approximate techniques are in good agreement with the ones obtained by integrating the 2PN equations. This shows that a complete account of all high-order post-Newtonian effects is usually not necessary for the determination of detection efficiencies. Based on our current astrophysical expectations, large tilt angles are not favored and as a result the decrease in detection rate varies rather slowly with respect to the black hole spin magnitude and is within 20–30% of the maximum possible values.

PACS numbers: 04.80.Nn, 95.75.-z, 95.85.Sz

## I. INTRODUCTION

Relativistic spin-orbit and spin-spin couplings can cause inspiraling binary compact systems containing neutron stars (NS) or black holes (BH), to precess, provided that at least one of the two spins is of significant magnitude and misaligned with respect to the orbital angular momentum. This precession leads to a periodic change of the orbital plane orientation and therefore modify the inspiral gravitational wave (GW) signal received by ground-based detectors. Currently binary inspiral searches with interferometric detectors, soon expected to be at optimal sensitivity, such as Laser Interferometric Gravitational Wave Observatory (LIGO) [1], VIRGO [2], and GEO600 [3], rely on sophisticated signal processing techniques to extract the signal from the intrinsic noise of the instruments. For binary compact objects, the best available linear filter is the well-known *matched-filtering* technique [4, 5]. For the maximum possible signal-to-noise ratio (SNR), this method requires the best possible *a priori* knowledge of GW signal waveforms to be used as templates. Schematically, the basic idea is to search for correlations between the output of the detector and the chosen family of templates. The maximum SNR is achieved when the signal coincides with one of the templates. If this is not the case, the loss in SNR can be measured by the *fitting factor* (FF), with relates the actual SNR to the maximum one by :

$$\left(\frac{S}{N}\right) = \text{FF} \times \left(\frac{S}{N}\right)_{\text{max}}, \quad (1)$$

as introduced in [6] (see also [7, 8], for more details on FF).

This paper represents the continuation of our group’s work, previously presented in [7, 8] (hereafter Papers I and II, respectively). This series is devoted to the study of precessing compact binaries and, more precisely to the effects of precession on the detectability of binary inspiral signals. If precession is not taken into account in the templates, it would cause a loss in SNR measured by  $\langle \text{FF} \rangle$  (averaged over source orientation) and consequently a decrease in

---

\*grandcle@phys.univ-tours.fr

†mia@northwestern.edu

‡vicky@northwestern.edu

§belczynski@northwestern.edu

detection rate by a factor  $\langle \text{FF} \rangle^3$ , assuming a homogeneous space distribution of the sources<sup>1</sup>. It has been shown in Papers I and II as well as in [10–12] that the detection rate could be greatly reduced (by up to an order of magnitude). It has also been known for some time now that this effect is more important in binaries with high mass ratios [12]. Therefore in this paper, we restrict ourselves to systems with a typical  $1.4M_\odot$  NS and a stellar-mass BH of  $10M_\odot$ . Let us note however, that according to [13], the most probable system to be detected by the first generation of detectors is not of that type, but rather consists of two black holes with mass ratio close to unity. Our current understanding of the physics of the interior of NS suggests that, in a binary system, the NS is not expected to have a spin of significant magnitude [14–16]. So we will assume that the most massive object, i.e. the BH, will carry all the spin. For this case where only one object is spinning, Apostolatos *et al.* (1994-1995) have derived an analytical approximation of the emitted waveform, valid up to 1.5 post-Newtonian (PN) order : the *simple precession* regime [6, 17]. For simplicity and computational efficiency, we will use this approximation, instead of integrating the full set of 2PN equations describing the dynamics of the system [18]. We will see that the results are very close to the ones obtained by Buonanno *et al.* using more detailed signals [10]. As in Papers I and II we will use the initial LIGO noise curve throughout the paper (values taken from table IV of [19]).

In a realistic data analysis pipeline, it is difficult to implement a search that uses the “full” precession waveforms as templates. Indeed such waveforms depend on a large number of parameters, typically ten (e.g., magnitude and orientation of the spins, orientation and position of the binary, etc), so that the computational burden to compute the cross-correlations with the output of the detector for all the possible values of the parameters is beyond the reach of current resources. To solve this problem, one can hope to find a family of “mimic” templates which depend on formally few parameters, but still leads to high FF values. Following and extending an initial proposal by Apostolatos [12], we presented, in Paper II, a strategy based on a hierarchical search, where successive corrections are applied to the phase of the templates. The final correction is the sum of an oscillatory term of the form proposed by [12] and several spike-like features, hence the name “spiky” templates.

Apart from the mass ratio, the effect of the precession modulation and hence the FF also depends on the spin magnitude of the most massive object (here the BH of  $10M_\odot$ ) and the tilt angle of this spin with respect to the orbital angular momentum. Until now none of the studies focused on the detectability of precessing binary inspiral have considered the astrophysical origin of the compact object spin magnitudes and orientations and their expected probability distributions. Clearly these will affect any *realistic* probability statement about the detectability of precession-modulated signals must take these into account. The physical origin of the tilts has been understood uniquely in the context of asymmetric compact object formation and the existence of supernova kicks [20–22]. Our current astrophysical understanding is well developed and allows theoretical predictions for the distribution of tilt angles among different populations of binary compact objects. On the other hand, the evolution of compact object magnetic field strengths is not as well understood, and therefore reliable probability distributions of spin magnitudes are difficult to calculate and the results are strongly model dependent.

The goal of this paper is twofold. In the first part of the paper (Sec. II), we examine more realistic precession waveforms (that include Thomas precession) and we show (Sec. II A) that the results are in excellent agreement with those obtained through numerical integration of equations that describe the orbital dynamics [10]. In section II B we point out our intriguing result that precession can, in some cases, help detection and increase the value of the signal-to-noise ratio. In the second part of the paper (Sec. III) we introduce, for the first time, the coupling between astrophysical predictions for the probability distributions of tilt angles with FF calculations and we obtain astrophysically relevant results for the detection rate degradation as a function of the compact object spin magnitude. Conclusions are presented in section IV.

## II. BEHAVIOR OF THE “SPIKY” TEMPLATES

### A. Dependence of FF on adopted precession inspiral signal

In Paper II, we proposed a technique to detect gravitational waves from precessing binaries, based on a three step hierarchical search. The first step was to just use the standard chirp templates, possibly including 2.5 PN corrections to the phase [23–25]. The second step was originally proposed by Apostolatos [12] and consists of the addition of a three parameter  $\mathcal{C}, B, \delta$  oscillatory term in the phase  $\mathcal{C} \cos(\mathcal{B}f^{-2/3} + \delta)$  (see Eq. (12) of [12]). Although this helped, we proposed to improve the efficiency of the procedure by searching for spike-like features (that we found appear in

---

<sup>1</sup> However, note that a recent study of the actual galaxy distribution in the nearby Universe shows that the slope-dependence of the number of sources within a certain distance is closer to 2.5 instead of 3 [9].

the residual phase after the two steps) in the phase as a third correction. Each spike depends on only two (rather well constrained) parameters (the position  $f_0$  and the width in frequency space, given by  $\sigma$ ) plus a boolean parameter (the sign  $\varepsilon = \pm 1$ ). More precisely the equation of a given spike is :

$$\begin{aligned} \text{If } f > f_0 \text{ then } P(f_0, \sigma, \varepsilon) &= \varepsilon \pi \left[ \sqrt{\left(1 - \frac{1}{(\sigma(f - f_0) + 1)^2}\right)} - 1 \right] \\ \text{If } f < f_0 \text{ then } P(f_0, \sigma, \varepsilon) &= \varepsilon \pi \left[ -\sqrt{\left(1 - \frac{1}{(\sigma(f - f_0) - 1)^2}\right)} + 1 \right]. \end{aligned} \quad (2)$$

The spikes are searched one by one until some convergence criterium is achieved. We refer the reader to Paper II for more details.

The results presented in Paper II were quite encouraging. However there is a number of points that still need some exploration. One of them is an important difference between the results presented in Paper II and the ones obtained in parallel and independently by Buonanno *et al.* [10]. Indeed, even though the two proposed schemes are completely different, the effects of precession should be the same, when using the standard (non-precessing) chirp signal. This was not the case : the lower curve of Fig. 12 of Paper II shows a fitting factor as low as 0.5 whereas, for the same system, Fig. 14 of [10] exhibits minimum values around 0.7. After some investigations, we determined that the main difference was coming from the assumption made in Papers I and II that the Thomas precession term in the simple precession formalism (given by Eq. (29) of [6]) is not important and could be ignored. As mentioned in Paper I, this term was believed to be mainly monotonic and well recovered by mismatching the parameters of the templates with respect to the physical ones of the signal. In contrast as we will see, the addition of the Thomas precession term (using 1.5 PN expressions for  $\dot{\omega}$ ) in the computation of the signal changes significantly the FF values.

Along with this main improvement we made a few other modifications. First, as already mentioned in Paper II, we have implemented the use of FFT techniques to find the maximum FF with respect to the time at coalescence  $t_c$ , at the first step of our procedure. By increasing the speed of the code, this modification enables us to explore a greater part of the parameter space. For example, contrary to Papers I and II, for which we used mainly Newtonian order for both the templates and the non-precessing part of the signal, in this work, we always use the 2.5 PN chirp signal, which depends on the total mass  $m_T = m_1 + m_2$  and the chirp mass  $\mathcal{M} = (m_1^3 m_2^3 / m_T)^{1/5}$ . We determined that using 1024 points for the FFT algorithm is sufficient to reach an accuracy of the order of 1% in identifying  $t_c$ .

We also modify some of the computational parameters involved in setting the templates database. More precisely, we increased the number of templates for both  $m_T$  and  $\mathcal{M}$ . In the previous papers, we determined those numbers by demanding that, in the cases *without* precession, the recovered FF would be  $\text{FF} \geq 0.97$ , which is similar to what is done for the searches with LIGO. On the other hand, it is possible that this criterion is not be sufficient for precise comparison with the work by Buonanno *et al.* [10]. Indeed in [10], the maximum FF is obtained by using a maximization algorithm and not by setting a grid of templates so that the precision is probably better than the one obtained by imposing  $\text{FF} \geq 0.97$  without precession. In order to make a meaningful comparison we increased the number of templates for the masses, requiring that the resulting precision of the FF was better than 1% , measured by convergence of the FF when increasing the number of templates (see Paper II for details). Once again, this leads to using too many templates especially compared to real searches. The new computational parameters for the masses are the following : the chirp mass (or the total mass) parameter is chosen between 80% and 115% (0.5% and 310%) of the signal masses. Those intervals are populated, in logarithmic scale, by 250 templates for the chirp mass and 350 for the total mass.

The last modification is a slight change in the criterion used for ending the search for spikes. In Paper II we used a relative convergence of the FF. However, for real searches, it is probably more convenient to adopt a criterion with respect to the SNR, given that the FF is not a very useful notion for noisy signals. Therefore we end the search for spikes when the SNR is modified by less than  $\Delta_{\text{SNR}} = 0.2$  between two consecutive spike fittings. Let us however note that this value is an important parameter. For real searches, in the presence of noise, preliminary results seem to indicate that it should be carefully chosen in order to avoid high false alarm rate. The precise effect of noise on the spikes is a subtle subject and is beyond the scope of this paper. Let us just mention that we have to deal with two competitive effects : on one hand, the smaller  $\Delta_{\text{SNR}}$ , the more spikes we find and so the higher the FF. On the other hand, the smaller the  $\Delta_{\text{SNR}}$  the more spikes are found, even in the presence of only noise, thus leading to a high false-alarm rate. This, once again, explains that this parameter must be chosen very carefully, given the specific behavior of the instrument noise.

In Figure 1 we show the calculated average  $\langle \text{FF} \rangle$  values as a function of the cosine of the misalignment angle  $\kappa \equiv \hat{\mathbf{S}} \cdot \hat{\mathbf{L}}$ , which is a conserved quantity, as long as simple precession is used. We consider only a maximally spinning BH (the spin measured as a fraction of  $m_1^2$  is  $S_1 = 1$ ). The circles and the dotted line denote the  $\langle \text{FF} \rangle$  obtained

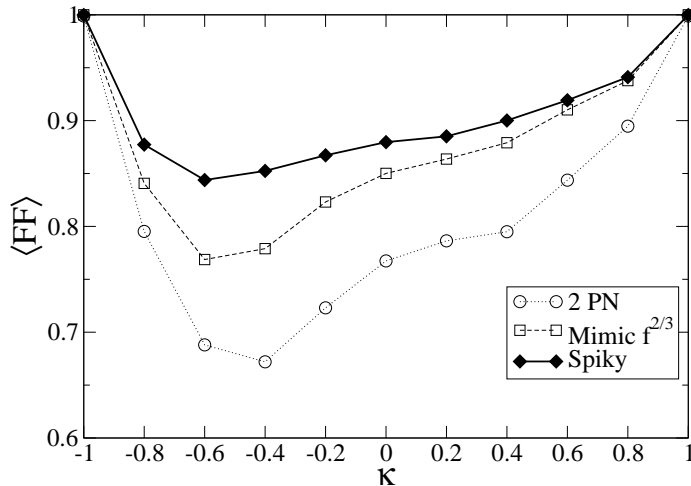


FIG. 1: Efficiency of the “spiky” templates in recovering the signal-to-noise ratio and increasing the inspiral detection rate. The circles and dotted lines correspond to the values obtained using the post-Newtonian templates. The squares and dashed lines correspond to the Apostolatos’ waveforms alone, and the filled diamonds and solid lines correspond to the combination of the Apostolatos’ correction and spiky templates. Each point represents the average  $\langle FF \rangle$  for 2,000 sets of source orientations. The curves are presented as a function of the cosine of the BH spin-orbit tilt angle :  $\kappa \equiv \hat{\mathbf{S}} \cdot \hat{\mathbf{L}}$ . We recall that the system is composed of two bodies :  $m_1 = 10M_\odot$  and  $m_2 = 1.4M_\odot$  with only  $m_1$  spinning. In this case the spin is maximum so that  $S_1 = 1$ .

by using only the standard templates. The most striking feature is that the curve is well above the values found in our Fig. 12 of Paper II. We have verified that two factors contribute to that : i) the use of PN templates instead of Newtonian ones ii) the addition of the Thomas precession term, the latter being the more important contribution, roughly by a factor of five. It is somewhat surprising that adding a term related to precession actually increases the FF, but this seems to be the case. The lower curve of Fig. 1 is now in very good agreement with the one labeled “SPAs” in Fig. 14 of [10], indicating that the simple precession regime is, indeed, a good approximation. Let us point out that the only significant difference is present for  $\kappa$  close to unity. This effect may seem surprising but is easy to understand and has actually little to do with precession. In the simple precession regime, when  $\kappa = 1$ , the signal coincides exactly with the chirp SPA signal (i.e. the modulations AM and PM in Eq. (10) of [17] are zero). So, for values of  $\kappa$  close to unity (i.e., small spin tilt angles), with a signal generated via simple precession, the FF should go to unity, as observed in Fig. 1. However, when using another way of generating the signal, that may not be true. Indeed, in [10], the signal is generated by numerically integrating equations for  $\omega$ , the spin and the orbital momentum. In the case  $\kappa = 1$  the only relevant equation is the one for  $\omega$  (i.e. Eq. (1) of [10]). The numerical solution coincides with the one used to derive the SPA waveform (see Eq. (7.11a) of [26] for example), only up to the given PN order. Higher order terms cause a small difference between the two waveforms, difference sufficient to explain an average FF as low as 0.8, even for  $\kappa = 1$ . All those considerations illustrate the very important fact that the detailed results can depend greatly from the exact formalism used to generate the precessing signal. Although we will restrict ourselves to simple precession in this paper, we plan to conduct a more extensive study of those effects in the future.

Figure 1 shows that, for low values of the spin tilt angle (i.e.,  $\kappa > 0.6$ ),  $\langle FF \rangle$  is close to 0.9 or higher. With such high values, the spikes are not as important in recovering the precession signal (this is why the solid and dashed curves almost coincide). However, for larger values of  $\kappa$ , the oscillatory correction begins to fail and the addition of the spikes leads to a significant gain, the maximum efficiency of the spikes being around  $\kappa = -0.5$ . After the three steps of the procedure, we are able to obtain fitting factors around 0.9, for all the possible values of the spin tilt angle. Such efficiency is comparable to the one shown by the alternative technique proposed by Buonanno *et al.* (see the top solid curve of Fig. (14) of [10]).

In order to convolve the results with astrophysical expectations (see Sec.III A), we have computed  $\langle FF \rangle$  values for the standard, non-precessing 2PN templates for a wide range of BH spin magnitudes. Results are shown in Fig. 2. The spin magnitude ranges from 0.1 (upper curve) to 1 (lower curve), with an increment of 0.1 from curve to curve. The computational parameters are the same than the ones used for Fig 1. Let us point out that the dependency

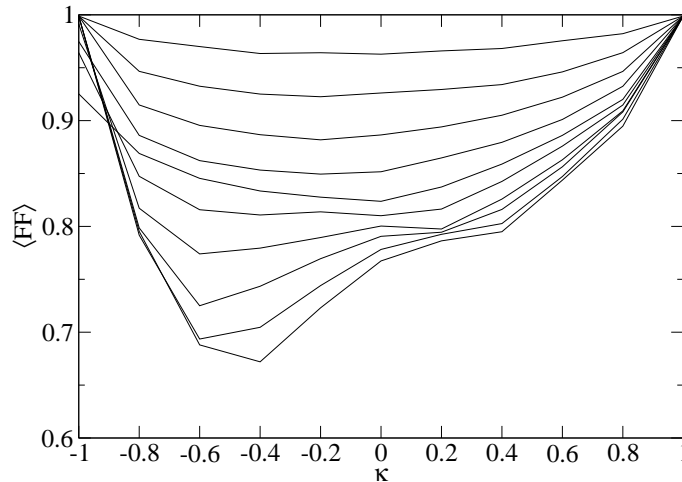


FIG. 2:  $\langle \text{FF} \rangle$  computed with the non-precessing templates, as a function of  $\kappa$ . The spin magnitude ranges from 0.1 (highest curve) to 1 (lowest curve), with a step of 0.1. Each point is the average  $\langle \text{FF} \rangle$  for 2,000 sets of source orientations.

on  $S$  is very moderate, at least for small tilt angles (i.e. high values of  $\kappa$ ). The curves that do not go to 1 when  $\kappa = -1$  (see  $S = 0.5$  for example) correspond to cases where the simple approximation breaks down. This is not a worrisome effect, given that such break-down only occurs for very misaligned configurations ( $\kappa$  close to  $-1$ ) which are very unlikely to occur in reality (see Sec. III A).

### B. Can Precession Help Detection ?

The efficiency of our procedure can also be presented without using the concept of FF, but rather by computing SNRs. Fixing the distance to 20Mpc, as an example, we simulate a set of 5,000 different binaries. Then we compute the SNR at which detection is achieved. Figure 3 shows the number of events for each particular interval of SNRs. The three different curves show the values after each step of our three-step procedure. Only the events with  $\text{SNR} \geq 8$  are presented (as this is our assumed detection limit). We can see that, even though the overall shape of the distribution does not change drastically, more and more events are detected when the successive corrections to the phase are added. The fraction of detected events are given by the percentiles in the legend-box of Figure 3. The improvement coming from Apostolatos' ansatz (Step II) and from the spikes (Step III) are both significant, the latter being half of the first one. Given the results of Fig. 1, we expect that the improvement comes mainly from systems with  $\kappa$  close to  $-0.5$  (remember that, in this section,  $\kappa$  is evenly distributed in  $[-1, 1]$ ; for astrophysical considerations on the distribution function of  $\kappa$ , see Sec. III).

The thick black curve of Fig. 3 represents the results using the same sets of orientations but setting  $S = 0$ . We first point out that the shape of the distribution is somewhat different from the same cases with precession (dotted line of Fig. 3). On one hand, for signals without precession there is a larger number of signals with high SNRs compared to those with precession, and this is quite intuitive. On the other hand, for low to moderate SNRs (8 to 10), there is significantly more systems with precession than without. This effect is so important that the number of events detected with precession, after the last step (54.2%) is very close to the one without precession (54.34%), even with FF values smaller than 1.

The conclusion is that there are systems for which the SNR with precession is higher than without. How is that possible ? Let us recall that the actual SNR is given by Eq. (1), where the  $(S/N)_{\text{max}}$  is given by the norm of the signal, i.e. by  $(W|W)^{1/2}$  (the optimum choice of scalar product is given by Eq. (2.3) of [27]; see also [4, 12, 17, 28] for details). Without precession the FF is 1 so, in order to get systems with higher SNR when  $S = 1$  than when  $S = 0$ , there must exist some systems for which  $(S/N)_{\text{max}}(S = 1) > (S/N)_{\text{max}}(S = 0)$ . In other words, at least for some systems, precession will *enhance* the strength of the gravitational wave signal. This can be physically understood as follows: consider a system which, when entering the frequency band of the detector, is oriented in the worst possible

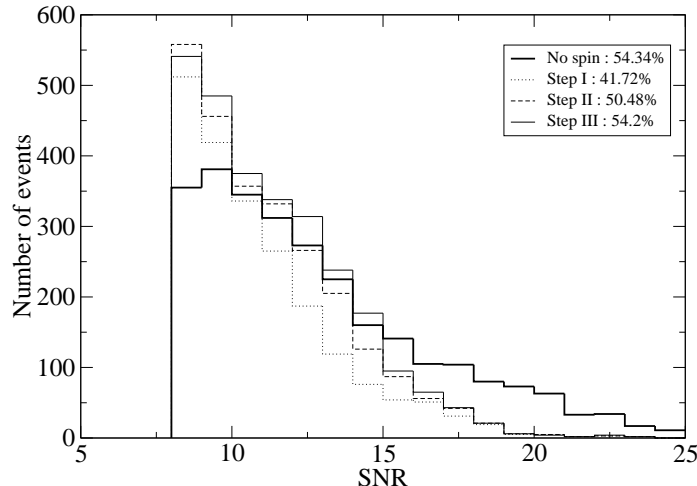


FIG. 3: Histogram of the signal-to-noise ratios at which the detection of 5,000 different orientations of a binary  $m_1 = 10M_\odot$ ,  $m_2 = 1.4M_\odot$  and  $S = 1$  is achieved. The dotted line denotes the results using the non-precessing standard templates, the dashed one after including the oscillatory term to the phase and the solid one after the addition of several spikes. The thick curve labeled *no spin* denotes the values of SNRs that are achieved by setting the spin of the BH to zero, keeping all the other parameters fixed. Only the detected events (i.e. those with  $\text{SNR} \geq 8$  are shown). The percentiles indicates the fraction of detected events with respect to the total number of binaries.

configuration, hence giving the lowest SNR possible. In the case  $S = 1$ , because of precession, the orientation of the orbital plane with respect to the detector is going to change and the system will no longer be in the worst possible orientation, hence will have higher SNR that what would be the case without precession. Of course there must also be systems for which the reverse is true, i.e. for which precession decreases the SNR.

To be more quantitative, we compute  $(S/N)_{\max}$  with  $S = 0$  and  $S = 1$  for a set of 5,000 configurations. Then we isolate the 72.4% of the systems that are detected in one case or the other, i.e. the systems for which either  $(S/N)_{\max}(S = 0) \geq 8$  or  $(S/N)_{\max}(S = 1) \geq 8$ . For those systems, Fig. 4 shows the distribution of the ratio of the two  $(S/N)_{\max}$ , in logarithmic scale. As expected, there is roughly half of the configurations for which precession enhances the strength of the signal and half for which it decreases it. However, let us note that the distribution is asymmetric so that the mean increase value is higher than the mean decrease one. This modification accounts for the fact that the distribution of SNR on Fig. 3 is different in the two cases  $S = 0$  and  $S = 1$  (respectively thick black curve and dotted curve). So to conclude with this effect, the “real” SNRs are modified by precession in two ways :

- the match between the templates and the signal is no longer perfect. This is measured by a decrease in FF.
- the  $(S/N)_{\max}$  are modified, which can either increase or decrease the strength of the signal.

In view of this understanding, let us come back to Fig. 3. The second effect is the same no matter what templates are used. The only difference between the various steps of our procedure is the fact that the FF increases. It is interesting to note that when using only the first two steps (non-precessing templates and Apostolatos’ ansatz) the net effect of precession is to reduce to number of systems detected. However, when the spikes are included, the decrease of FF is sufficiently small to be compensated by the enhancement in  $(S/N)_{\max}$ , causing roughly the same number of systems to be detected than in the case  $S = 0$ . However, it is true that for some events the  $(S/N)_{\max}$ , hence the actual SNR, decreases, as it seems to be the case for the systems with very high SNRs. To summarize, we have illustrate the fact that, by modifying the signal, precession, if correctly accounted for by the templates (i.e. with sufficiently high FF), can help recovering the same number of detection than with  $S = 0$ . From this point of view, it seems that, in some cases, precession could help the detection of inspiral signals.

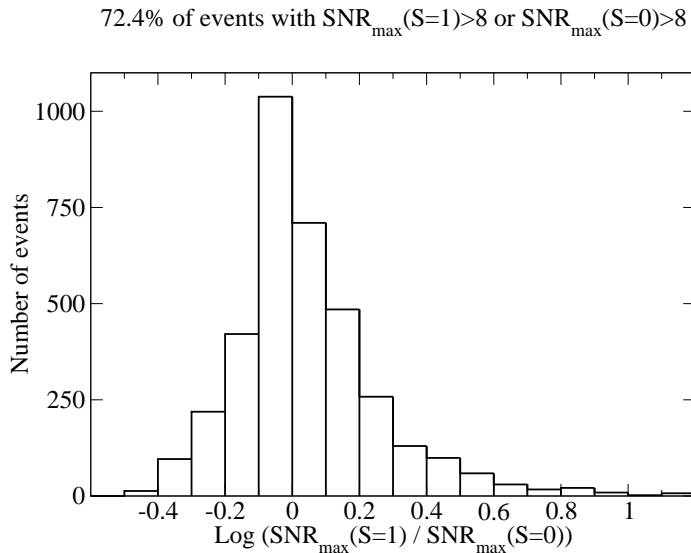


FIG. 4: For events that are detected at least in one of the two cases  $S = 0$  or  $S = 1$ , this histogram shows the distribution of the ratios of the two  $(S/N)_{\text{max}}$ , in logarithmic scale. This illustrates the fact that, depending on the actual orientation of the system, precession can either increase or decrease the strength of the signal.

### III. SPIN TILTS IN DOUBLE COMPACT OBJECTS

#### A. Spin Tilt Astrophysics

Inspiral binaries have already been detected in our Galaxy and are known as relativistic binary pulsars (the Hulse-Taylor systems PSR B1913+16 being the prototype [29]). All the known double compact objects with coalescence lifetimes shorter than the Hubble time consist of two neutron stars or a neutron star and a white dwarf (their inspiral is relevant to the planned space mission LISA [30, 31]). Nevertheless current theoretical understanding of binary compact object formation (consistent with the binary pulsars) undoubtedly leads to the prediction for the existence of close binaries with a NS and a BH, and for the majority of models of binary BHs (e.g. [35]; hereafter BKB). Their formation is understood as the outcome of many different binary evolutionary sequences all of which involve a long chain of phases of mass and angular momentum transfer between binary components (the progenitors of the compact objects) as well as mass and angular momentum losses from the binaries (see BKB). Of all these evolutionary links there is only one that is believed to be the origin of spin-orbit misalignments, at least for binaries in the galactic field, i.e. not in globular clusters: the asymmetric collapse of massive stars that imparts a randomly oriented recoil velocity (known as “kick”) to the nascent compact objects, which affects the binary orbital characteristics and depending on its magnitude and direction can cause the orbital plane to tilt from its pre-collapse orientation. Observational evidence in support of NS kicks has accumulated over the past two decades from a variety of sources, most important being the large measured space velocities of pulsars [32]. For a couple of binary pulsar systems (one of them being the Hulse-Taylor binary), careful timing and polarization pulsar measurements have provided evidence in support of a non-zero tilt angle between the pulsar spin axis and the orbital angular momentum axis. Such misalignments have been theoretically interpreted as the result of asymmetric kicks and have been used to provide quantitative constraints on kick magnitude and orientation [20, 21].

This basic theoretical understanding has already been used in a preliminary study of the tilt angle distributions expected for BH-NS and BH-BH binaries and their general implications for the reduction in detection rate, if non-precessing templates are used in GW inspiral searches (see Kalogera [33], hereafter K00). As discussed in K00 in more detail, the tilt-angle calculation is possible in part because of two main evolutionary factors:

- The complicated evolutionary history of binary compact objects includes multiple phases of strong tidal interactions and mass-transfer phases. The spins of the binary components are expected to be aligned with the orbital angular momentum axis just prior to the formation of the second compact object because of the exchanged angular momentum between the stars and the orbit through these tidal interactions. Therefore, even if earlier in the evolution of the binary compact object progenitors spins were misaligned, all momenta axes are expected

to be aligned just prior to the second supernova explosion.

- In a BH-NS binary the BH is expected to form from the initially more massive star in the binary. Since more massive stars evolve faster, the BH is expected to be formed first and its spin is expected to be aligned with the orbit just prior to the second explosion. The NS formed in this second explosion is expected to receive a natal kick, which can result in the post-explosion orbital plane being tilted with respect to the pre-explosion orbital plane. Given the extremely small cross section of the BH, its spin remains unaffected and aligned with the pre-explosion orbital angular momentum, and hence *misaligned* with respect to the orbital angular momentum axis of the newly formed double compact object<sup>2</sup>.

K00 developed a basic scheme for the quantitative modeling of the orbital dynamics during an asymmetric explosion and the resultant distributions of orbital-plane tilt angles, under the assumption of *circular* pre-supernova orbits. Based on the above considerations these tilt angles are the misalignment angles between the BH spin and the orbital angular momentum axis, right after the formation of the double compact object. Furthermore, it has been shown that the time-scale for any evolution in the tilt angle due to spin-spin and spin-orbit couplings is much longer than the age of the universe [34]. Consequently, the post-explosion tilts are expected to be preserved during the inspiral phase and to be relevant at the very late phases when the GW frequencies enter the detection bands of ground-based interferometers ( $\gtrsim 40$  Hz for initial LIGO, for example). The results in K00 indicated that BH-NS systems can have significant (up to 70% of the systems with tilt angles in the range  $50^\circ - 100^\circ$ ) tilt angles, whereas heavier BH-BH systems with typically smaller kick magnitudes tend to have very small tilt angles (more than 90% of the systems with a tilt angle smaller than  $30^\circ$ ).

Apart from the assumption of circular pre-explosion orbits, K00 adopted a number of simplifications: (i) tilt distributions were calculated for a few specific sets of pre-explosion binary parameters (component masses and orbital separations) without taking into account the probability distributions of pre-explosion binary characteristics, given the prior evolutionary history of the systems; (ii) the tilt distributions were not convolved with detailed calculations of FF and its dependence on tilt angle and spin magnitude. Here we present a more sophisticated analysis that expands the preliminary study in K00 in three major ways: (i) we use binary compact object population models that account for the full evolutionary history of binaries from their formation as primordial binaries in the Galaxy until double compact objects form; these population models provide a detailed record of the distribution function of binaries in their parameter space (4-dimensional: two masses, orbital semi-major axis, and eccentricity) just prior to the second explosion that introduces the BH spin tilt; (ii) we expand the mathematical derivation of K00 to account for the general case of eccentric binaries; (iii) we convolve our astrophysical predictions for tilt angle distributions with our results for the FF values as a function of spin tilt and magnitude. This allows us to derive astrophysically “weighted” FF as a function of spin magnitude and examine the systematics of our results for different population models.

## B. Spin Tilt Calculations and Results

Although many of the details of binary evolution are not well understood, the current general understanding (based both on theoretical stellar evolution calculations and comparisons with a very wide range of different binary types) is quantitative enough to allow the statistical modeling of binary populations and the calculation of probability distributions of all physical parameters of interest. For a wide variety of scientific problems, such *population synthesis* calculations have been used for more than 20 years now, especially in the area of binaries with compact objects [36]. Most commonly Monte Carlo methods are used to generate a large number ( $10^6 - 10^7$ ) of primordial binaries with physical properties that follow certain distribution functions. The evolution of each binary is independent of the other (since in the Galactic field the interaction time is longer than the age of the Milky Way) and is modeled through long sequences of evolutionary phases, until the end of the binary’s lifetime. Throughout the calculation the binary characteristics are calculated self-consistently. The overall normalization of the models is fixed by observational constraints on the supernovae and the star formation rates of the galaxy.

For our calculations we use the code *StarTrack* that was originally developed by Belczynski et al. (2002) specifically for the study of binary compact object coalescence rates and physical properties (BKB). The code, results, and comparisons with earlier work by other groups have been described extensively in BKB, so we will not repeat the astrophysical description here. We further note that in the past year the population synthesis code has been

---

<sup>2</sup> Similar considerations hold for a BH-BH binary, where the NS is typically replaced by the least massive of the two BHs. However, note that it has been recently shown [13] that relatively massive BH-BH with mass ratios close to unity have the highest detection probability and that such systems are not expected to receive significant kicks (if any).



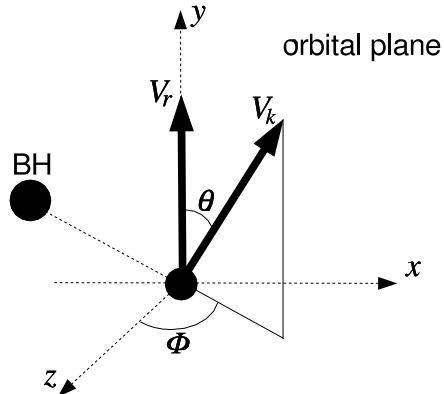


FIG. 5: Orientation of the binary. The  $(x, y)$  plane is the orbital one,  $\vec{e}_y$  being in the direction of  $\vec{V}_r$  and  $\vec{e}_z$  in the one of the orbital momentum. The orientation of the kick velocity  $\vec{V}_k$  is given by the two angles  $\theta$  and  $\phi$ . Note that, contrary to Fig. 1 of K00, the BH is no longer in the x-direction in the case of eccentric orbit.

modified with special focus on the treatment of mass-transfer phases: a new, computationally efficient scheme has been developed that, for the first time allows the calculation of mass-transfer rates and binary evolution through mass-transfer phases that have been carefully tested against results of detailed stellar evolution codes and are in very good agreement [37]. Using this updated code we have studied the properties of double compact objects using a subset of the set of models considered by BKB. We find that the results from the updated version are qualitatively identical to the early models (presented in detail in BKB) and, in terms of the tilt-angle distributions, quantitatively similar but with noticeable differences (typically the new models have a somewhat larger fraction of binaries formed with tilt angles in excess of  $10^\circ$ ).

In what follows we consider the results from two models already presented in BKB: the standard model A and the model E1 (with  $\alpha_{\text{CR}}\lambda = 0.1$ ). These have been selected because they provide the widest variations in results in terms of tilt-angle distribution functions. The details of the physical parameters in each model and the reasons for their choice are described in detail in BKB. We avoid the repetition here, since, as we will see, the astrophysical motivation and details are not important for the results and conclusions from this study. However we do describe here the calculation of the tilt angles for *eccentric* pre-explosion orbits, since the derivation does not appear anywhere else in the literature.

We adopt a reference frame analogous of the one used in K00. However, we need to slightly modify it to take into account eccentric orbits. The axes are defined as follows.  $\vec{e}_y$  lies into the direction of the initial velocity  $\vec{V}_r$  of the progenitor,  $\vec{e}_z$  in the direction of the orbital momentum and we have  $\vec{e}_x = \vec{e}_y \times \vec{e}_z$ . Then, the  $(x, y)$  plane is the orbital one. This system is the same than the one used in K00 except that, for eccentric orbits, the BH is no longer always in the x-direction. Let us call  $A_0$  the semi-major axis of the orbit and  $r$  the separation at the moment of explosion. We call  $V_c$  the value of  $V_r$  when  $r = A_0$  (the subscript c stands for circular). The magnitude of the kick velocity is given by  $V_k$  and its orientation by the two angles  $\theta$  and  $\phi$  (cf. Fig. 5).

The velocity  $\vec{V} = \vec{V}_r + \vec{V}_k$  of the NS, after explosion is then given by (see also [38], by replacing  $\phi \rightarrow \pi/2 - \phi$ ) :

$$\frac{V_x}{V_c} = u_k \sin \theta \sin \phi \quad (3)$$

$$\frac{V_y}{V_c} = (V_r/V_c) + u_k \cos \theta = \sqrt{2A_0/r - 1} + u_k \cos \theta \quad (4)$$

$$\frac{V_z}{V_c} = u_k \sin \theta \cos \phi \quad (5)$$

where we have defined  $u_k \equiv V_k/V_c$ .

As in K00, the tilt angle  $\omega$  can be calculated by considering that it is the angle between two vectors: the initial velocity  $\vec{V}_r$  and the projection  $\vec{V}_p$  of  $\vec{V}$  onto the plane  $\phi = 0$  (note a typo in K00). This leads to :

$$\kappa \equiv \cos \omega = \frac{\sqrt{2A_0/r - 1} + u_k \cos \theta}{\sqrt{(\sqrt{2A_0/r - 1} + u_k \cos \theta)^2 + (u_k \sin \theta \cos \phi)^2}} \quad (6)$$

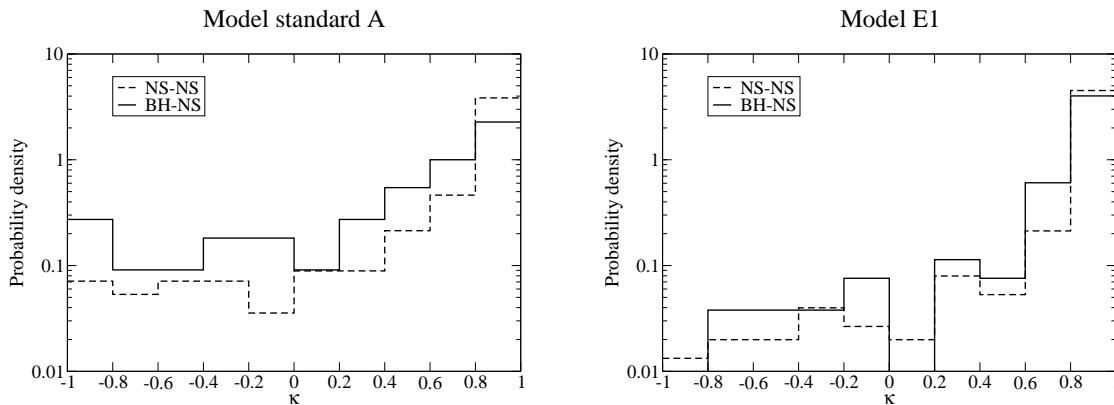


FIG. 6: For the models A and E1, the probability distribution of the tilt-angle  $\kappa$  is shown. On both plots, the solid curve denotes the results for BH-NS systems and the dashed one the NS-NS systems.

In the case of a circular orbit, for which  $A_0 = r$ , we recover Eq. (3) of K00. The radius  $r$  is chosen proportionally to the time spent at each point of the orbit before the explosion.

In Fig. 6 our results for the probability distribution of  $\kappa$  are shown for the two population models. Each panel shows the distribution for binaries of types NS-NS and BH-NS. We did not show the BH-BH binaries because the statistics we got was too low to be meaningful. In general it is evident that it is very difficult to tilt the orbital plane by large angles. It can be shown mathematically that the tilt angle increases as the magnitude of the kick velocity component perpendicular to the pre-explosion orbital plane ( $\vec{V}_k \cdot \vec{e}_z$ ) increases too. However, as this quantity increases, statistically so does the total kick magnitude. On the other hand, the latter has the effect of disrupting the binary and hence *not* forming a binary compact object. This is the physical reason for why low tilt angles are more favored: they occur in systems that have avoided disruption.

The results from the two systems behave in a rather similar manner. The probability density drops rapidly of 1-2 orders of magnitude between  $\kappa = 1$  and  $\kappa = 0$  and remains relatively constant afterwards ( $\kappa < 0$ ). The main difference between the two models is that it is easier to get large tilt angles in the standard model A than for E1. This effect is very noticeable and, as we will see, will reflect on the  $\langle \text{FF} \rangle$  distribution. For both models, it seems that the BH-NS systems are slightly easier to tilt than the NS-NS ones. This is another reason, apart from the fact that precession is more important for system with very different masses, to consider only precession for BH-NS systems.

### C. Astrophysically Relevant Fitting Factors

In Sec. II A  $\langle \text{FF} \rangle$  are calculated for a representative BH-NS binary and for a grid of BH spin magnitudes  $S$  and spin tilts  $\kappa$ . Here we use the astrophysical model predictions for the distribution of  $\kappa$  to derive “*astrophysically weighted*” fitting factors  $\langle \text{FF} \rangle_{\text{astro}}$  that depend only on the BH spin magnitude and are defined as:

$$\langle \text{FF} \rangle_{\text{astro}}(S) = \int_{-1}^1 f(\kappa) \langle \text{FF} \rangle(\kappa, S) d\kappa. \quad (7)$$

In Fig. 7 we show the derived astrophysical  $\langle \text{FF} \rangle_{\text{astro}}^3$  values as a function of the BH spin magnitude. The variation across the range is moderate and  $\langle \text{FF} \rangle_{\text{astro}}^3$  values are typically  $\geq 0.7$ . They depend only moderately on  $S$  and on the details of the population models. As expected from the probabilities shown on Fig. 6, the model E1 exhibits values above the standard one by about 20%. The decrease in detection rate, if precession is ignored in the inspiral templates, is only moderate and about 20-30%. This result is the outcome of a balance between the fact that the lowest  $\langle \text{FF} \rangle$  occur for  $\kappa \sim -0.5$  (see. Fig. 2) and that there is only a low probability for BH-NS to have such large tilts (see Fig. 6). Figure 7 also shows the values obtained when using both Apostolatos’ waveforms (empty symbols) and the “spiky” templates (filled symbols), for model A (the squares) and E1 (the diamonds). We can see that the improvement induced by the spikes is not very important in this case. This is not surprising, given that the spikes are efficient in the region  $\kappa \simeq -0.5$  which is a value which is not favored at all by astrophysical models (see. Fig. 6). The inclusion of the mimic templates is also more efficient for the model A than for E1 and is easily explained by the fact that the model A produces significantly more systems with large values of the misalignment angle.

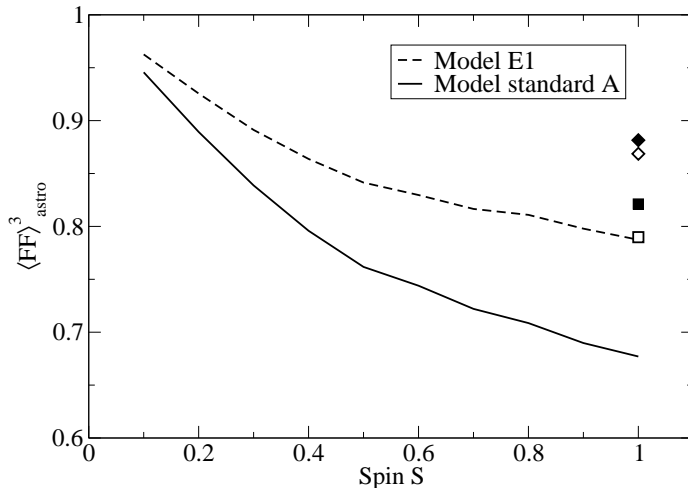


FIG. 7: Reduced detection rate, given a probability distribution for  $\kappa$ . The system is composed of a black hole and a non-spinning NS.  $\langle \text{FF} \rangle_{\text{astro}}^3$  is presented for both models, as a function of the spin of the black hole. The empty square (diamond) denotes the value for Apostolatos’ templates, for model A (E1) and the filled square (diamond) the value using the “spiky” templates for model A (E1).

#### IV. CONCLUSIONS

The first part of this paper is the natural continuation of previous work and is devoted to a more detailed study of various precessing effects. We used more detailed signals than in Papers I and II, always generated by the simple precession formalism, but using 2PN expressions for the non-precessing terms and including Thomas precession. It turns out that those two modifications significantly increases the values of  $\langle \text{FF} \rangle$ , compared to what was previously found, which is somewhat surprising and counter-intuitive. On the other hand, the results are now in very good agreement with the ones obtained by [10].

Using those more detailed signals, we then explored the efficiency of the family of “spiky” templates proposed in Paper II. The values of  $\langle \text{FF} \rangle$  being higher, the spikes are less efficient than previously found. However, the overall procedure still leads to values of  $\langle \text{FF} \rangle$  comparable to the ones found by [10] (see however recent work in [11], where even higher  $\langle \text{FF} \rangle$  are achieved). Using our “spiky” templates we then computed “real” SNRs, fixing the distance of the binary to 20Mpc. In doing so, we were able to illustrate and quantify the fact that precession can, in some cases, help detection. This is due to the fact that, even if  $\text{FF} < 1$ , the strength of the signal can be enhanced by precession. In future work, we plan to see how the efficiency of our procedure is modified by using more complicated signals, mainly by dropping the adiabatic approximation. We also plan to explore the behavior of the “spiky” templates in the presence of noise.

In the second part of this paper, for the first time, we explore the effect of precession on gravitational-wave inspiral searches in view of the most current understanding of the physical origin of spin-orbit tilt angles and associated predictions for the probability distributions of tilt angles. Taking into account detailed models for the full evolutionary history of close binary compact objects we calculate the probability distributions of tilt angles for different types of systems and find that the strong majority of tilts are smaller than  $\simeq 60^\circ$ . This is mainly due to the requirement that binaries remain bound after compact object formation *and* in a tight orbit (with coalescence times shorter than the Hubble time).

We use the predictions for tilt-angle distributions to calculate “astrophysically-weighted” fitting factors  $\langle \text{FF} \rangle_{\text{astro}}$  as a function of black hole spin magnitude. We find that most probably Nature protects us from a large decrease of the inspiral detection rate in the case that non-precession templates are used: for a wide range of binary evolution models, the decrease factors of detection rates turn out not to depend strongly on the spin magnitude and they remain rather well restricted within 20 – 30% of the maximum possible.

The implication of our results on the astrophysical expectations of tilt angles is that precession effects may not as important as previously thought for the searches of gravitational-wave inspirals. However, precession in principle

can still be important, if larger tilt angles are more favored than currently thought. Given the fact that the current understanding of binary compact object formation is far from perfect and that the anticipated detection rates for first-generation interferometers may be low, it is probably best to still account for precession effects in the best way possible in gravitational-wave data analysis.

### Acknowledgments

This work is supported by NSF Grant PHY-0121420. V.K. also acknowledges financial support from the David and Lucile Packard Foundation, in the form of a Fellowship in Science and Engineering.

- 
- [1] A. Abramovici *et al.*, *Science* **256**, 325 (1992).
  - [2] B. Caron *et al.*, *Nucl. Phys.* **B54**, 167 (1997).
  - [3] K. Danzmann, in *Gravitational Waves Experiments*, eds. E. Coccia, G. Pizzella and F. Ronga, World Scientific, Singapore (1995).
  - [4] C.W. Helstrom, *Statistical Theory of Signal Detection*, 2nd edition, Pergamon Press, London (1968).
  - [5] B.J. Owen and B.S. Sathyaprakash, *Phys. Rev. D* **60**, 022002 (1999).
  - [6] T.A. Apostolatos, C. Cutler, G.J. Sussman and K.S. Thorne, *Phys. Rev. D* **49**, 6274 (1994).
  - [7] P. Grandclément, V. Kalogera and A. Vecchio, *Phys. Rev. D* **67**, 042003 (2003).
  - [8] P. Grandclément and V. Kalogera, *Phys. Rev. D* **67**, 082002 (2003).
  - [9] P. Nutzman, V. Kalogera, S. Finn, C. Hendrickson, K. Belczynski, *ApJ*, submitted.
  - [10] A. Buonanno, Y. Chen and M. Vallisneri, *Phys. Rev. D* **67**, 104025 (2003).
  - [11] Y. Pan, A. Buonanno, Y. Chen and M. Vallisneri, submitted to *Phys. Rev. D*, preprint: gr-qc/0310034 (2003).
  - [12] T.A. Apostolatos, *Phys. Rev. D* **54**, 2421 (1996).
  - [13] T. Bulik, D. Gondek-Rosinska and K. Belczynski, submitted to *MNRAS*, preprint: astro-ph/0310544, (2003).
  - [14] J.H. Taylor and J.M. Weisberg, *APJ* **253**, 908 (1982).
  - [15] A. Wolszczan, *Nature* **350**, 688 (1991).
  - [16] L. Bildsten and C. Cutler, *ApJ* **400**, 175 (1992).
  - [17] T.A. Apostolatos, *Phys. Rev. D* **52**, 605 (1995).
  - [18] L.E. Kidder, *Phys. Rev. D* **52**, 821 (1995).
  - [19] T. Damour, B.R. Iyer and B.S. Sathyaprakash, *Phys. Rev. D* **63**, 044023 (2001) .
  - [20] V.M. Kaspi, M. Bailes, R.N. Manchester, B.W. Stappers and J.F. Bell, *Nature* **381**, 584 (1996).
  - [21] N. Wex, V. Kalogera and M. Kramer, *ApJ* **528**, 401 (2000).
  - [22] S. Portegies-Zwart and L. Yungler'son, *A&A* **332**, 173 (1998).
  - [23] B.S. Sathyaprakash and S.V. Dhurandhar, *Phys. Rev. D* **44**, 3819 (1991).
  - [24] S.V. Dhurandhar and B.S. Sathyaprakash, *Phys. Rev. D* **49**, 1707 (1994).
  - [25] R. Balasubramanian and S.V. Dhurandhar, *Phys. Rev. D* **50**, 6080 (1994).
  - [26] C.M. Will and A.G. Wiseman, *Phys. Rev. D* **54**, 4813 (1996).
  - [27] C. Cutler and E.E. Flanagan, *Phys. Rev. D* **49**, 2658 (1994).
  - [28] L.S. Finn, Written version of lectures given at XXVI SLAC Summer Institute on Particle Physics *Gravity: From the Hubble Length to the Planck Length*, gr-qc/9903107, (1998).
  - [29] R.A. Hulse and J.H. Taylor, *ApJ* **195**, L51 (1975).
  - [30] Lisa NASA Homepage, <http://lisa.jpl.nasa.gov>
  - [31] Lisa ESA Homepage, <http://sci.esa.int/hole/lisa>
  - [32] E.P.J. van den Heuvel and J. van Paradijs, *ApJ* **483**, 399 (1997).
  - [33] V. Kalogera, *ApJ* **541**, 319 (2000).
  - [34] F.D. Ryan, *Phys. Rev. D* **52**, 3159 (1995).
  - [35] C. Belczynski, V. Kalogera and T. Bulik, *Apj* **572**, 407 (2002).
  - [36] R.J. Dewey and J.M. Cordes, *ApJ* **321**, 780 (1987).
  - [37] C. Belczynski, V. Kalogera, F.A. Rasio and R.E. Taam, *ApJ*, to be submitted.
  - [38] J.G. Hills, *ApJ* **267**, 322 (1983).